# SALT WEATHERING OF BRICK WALLS

Salman Shahidi
*CNRS, Orléans, France*

Keywords: Natural Phenomena, Weathering Phenomena, 3D Texture Synthesis, Displacement Mapping.

Abstract: Human made buildings and constructions are very dependent upon various weathering phenomena, resulting in complex appearances and patterns that vary with time and environment. Handling such complexity is important in computer graphics in order to improve the realism of images. This difficult work is usually done by hand by designers and can lead to non-plausible results. Another way to tackle this problem is to provide new aging algorithms. Among a large number of weathering, salt weathering results in important visual changes affecting widely used materials: bricks and mortars. In this paper, we present a method to generate the texture of deformed and eroded masonry face by efflorescence. To avoid complex and unintuitive formulations while keeping plausible results, we chose a physically-inspired model. Moreover, in order to keep an important artistic control, it is possible for the user to create weathered textures in preferential masonry zones, leading to a great variety of different patterns. First, we synthesize a masonry (brick/mortar) solid texture. Next, we add the effects of efflorescence and sub-florescence using a specific algorithm accounting for regular crystallized or eroded surface masonry by displacement mapping. In addition, to model very strong weathering effects on building walls, we apply a simple geometry modification method to modify the surface before its rendering.

## 1 INTRODUCTION

Mortar and bricks are two important and widely used construction materials. Their appearance is often greatly affected by environmental and time dependent phenomena such as salt deposition and crystallization, which lead to their deterioration. therefore, to make realistic images of human constructions, we should take into account these imperfections to avoid non-realistic smooth texture shown in usual synthesized image. This issue is increasingly investigated in computer graphics, using new techniques in all computer graphics fields (modeling, rendering, animating). These works have resulted in generic methods as well as specialized techniques focusing on a specific weathering process. Due to the visual importance of brick and masonry in our environment, we propose to treat this specific weathering phenomenon by a specialized technique. An image gallery of weathering problem in the course of time and salts on the masonry is shown in Figure 1. The alterations are clearly visible on the surfaces.

The goal of this work is to automatically generate the most common weathering effects on brick constructions. We focus specifically on deformed crystallized masonry and structural damage such as crumbling and erosion. For this, we propose to use a masonry surface model built upon solid texturing (Peachey, 1985; Perlin, 1985). Solid texturing is well suited for patterns as for efflorescence and erosion on the masonry, which are intrinsically three-dimensional.

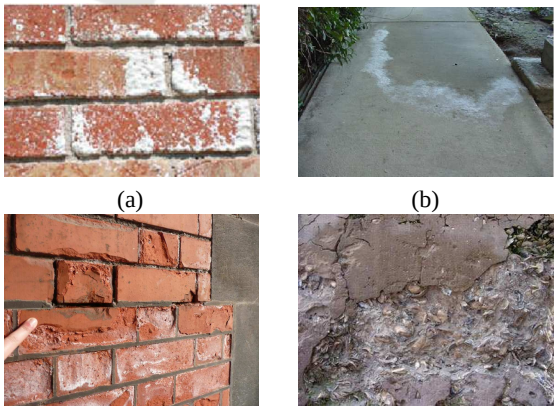


Figure 1: Examples of weathering effects. (a) Crystallization on a brick wall. (b) Thin efflorescence on a homogeneously cement. (c) and (d) present damages dues to crystallization that occurs inside the material near the surface.

Shahidi S..
SALT WEATHERING OF BRICK WALLS.
DOI: 10.5220/0003807600070015
In *Proceedings of the International Conference on Computer Graphics Theory and Applications* (GRAPP-2012), pages 7-15
ISBN: 978-989-8565-02-0

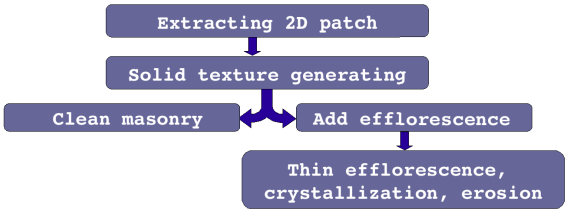


Figure 2: Flowchart of the system. We adopt the solid texture method to synthesize a clean masonry. We make a discrete 3D block B of colors of size $N^3$. The block B is produced by extruding and perturbing an input 2D image patch, representing a view of the desired 3D texture. To synthesize masonry, we can apply the block of colors B to a masonry silhouette.

The overall design of our system is organized according to the flowchart shown in Figure 2. The first task is to extract a patch from real photo. To obtain a discrete 3$D$ block $B$ of size $N^3$ we extrude this patch along its perpendicular direction to synthesize the solid texture of a clean brick. In order to keep the realistic texture, we simply perturb the extrusion process by Perlin-noise (Perlin, 1984). Texturing a brick shape mesh by solid texture $B$, results in a formation of a clean brick without weathering effects. By adding different forms and integrities of salt colors on a clean brick, then using a specific surface degradation method, we can generate different efflorescence and erosion patterns on masonry.

The next section gives a brief overview of the previous and related work about surface deterioration synthesis, followed in section 3 by an overview of the physics of salt crystallization leading to masonry surface damage. Section 4, deals with simulating of salt crystallization on the surface, then section 5 shows comparisons between real and synthesized brick walls. Finally, in section 6 conclusions and future work are given.

## 2 PREVIOUS AND RELATED WORK

Becket and Badler handled imperfections of surface by employing a fractal based texture synthesis technique (Becket and Badler, 1990). Blinn (Blinn, 1982) and Hsu (Hsu and Wong, 1995) have studied dusty surfaces, and Miller (Miller, 1994) has investigated tarnished surfaces with accessibility shading algorithms. Wong et al. have proposed a geometric method to represent patinas, dust, and peeling (Wong et al., 1997). Paquette et al. have proposed to handle geometric defects due to impacts (Paquette et al., 2001); they also investigated peeling and crackling of paint (Paquette et al., 2002). Dorsey et al. (Dorsey and Hanrahan, 1996) proposed a model to take into account dirtiness brought onto surfaces by flow processes, as well as weathered stones (Dorsey et al., 1999). Merillou et al. have studied destructive corrosion (Merillou et al., 2001). Bosch et al. (Bosch et al., 2004) studied the scratches on surfaces. Desbenoit et al. studied the growth of lichens (Desbenoit et al., 2004).

Other techniques try to handle the weathering phenomena in a more global way, often related to measurements (Lu et al., 2007) or texture synthesis (see for example (Cutler et al., 2002)). Note that a survey on aging and weathering phenonema has recently been proposed in (Merillou and Ghazanfarpour, 2008).

Concerning the aging of buildings only a few studies have been specifically proposed. In (Shahidi et al., 2005), we have presented a model to synthesize thin efflorescence on fired-clay bricks without accounting for larger scale efflorescence, and Merillou et al. (Merillou et al., 2010) have studied the effects of atmospheric pollution. The present work belongs to this specific topic, increasing the available building aging techniques.

## 3 PHYSICS OF SALT CRYSTALLIZATION

We limit our model to a physical deterioration whose damaging effects are linked with wetting and drying cycles on the front walls. Drying/wetting experiments were performed on various types of fired-clay brick by Pel et al. (Pel et al., 2004). In all drying experiments, it was observed that the moisture profiles were almost homogeneous, and within the time of these experiments (i.e. up to 14 days), no receding drying fronts were observed. Figure 3 shows a diagrammatic representation of the drying process with one drying side (valid for fired clay bricks and mortar) that saturated with a salt solution. During the drying process, moisture will be transferred onto the drying surface. The transport of moisture for the one-side surface drying problem in time $t$ and position $x$ from drying surface, can be described by a nonlinear equation of diffusion (see also (Huinink et al., 2002; Pel et al., 2004)): $\frac{\partial \theta}{\partial t} = \frac{\partial}{\partial x}\left[D(\theta)\frac{\partial \theta}{\partial x}\right]$, where $\theta(m^3m^{-3})$ presents the volumetric liquid moisture content, $D(\theta)(m^2s^{-1})$ is the iso-thermal moisture diffusivity. During the drying, the ions (e.g., $Na$ ions of $NaCl$ salt solution source) are advected to the drying surface and the salt concentration slowly increases to saturate. At this

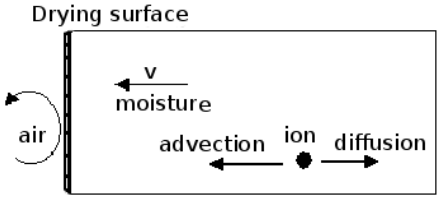


Figure 3: Diagrammatic representation of drying/wetting process for the materials with one-side drying face. Illustration adapted from work of Pel et al. (Pel et al., 2004).

point additional advection will result in crystallization at the top of the sample (drying surface), which is observed as a white efflorescence.

The wetting and drying cycles are the major cause of crystallization that leads to masonry deterioration (Bucea et al., 2005; Nehdi and Hayek, 2005). As drying/evaporation occur at the masonry surface, salts crystallize out of solution producing the white crystals known as efflorescence. These white crystals can change color, reflection properties, and geometry of the surface. Hidden salt crystallization that occurs below the masonry surface within the pores is called sub-florescence, leading to often strong deterioration of the masonry. This may be visually observed as cracking, spalling patterns, deflection, stains, and erosion. Table 1 shows an observation of these attacks by different salts (normally sodium sulphate and sodium chloride) in laboratory conditions after 3 and 48 months, which is representative of real conditions in long periods (Hees and Brocken, 2004).

Table 1: Overview of damages after 3 months and 48 months (tested by Hees and Brocken (Hees and Brocken, 2004)).

| | Sodium Sulphate | Sodium Chloride |
|---|---|---|
| 3 months | efflorescence, delamination, crumbling | efflorescence |
| 48 months | efflorescence, push out, delamination, crumbling | efflorescence, crumbling, slit crack |

Crystallization on brick wall accumulates with repeated wetting and drying cycles of the brick (Benavente et al., 2004; Pel et al., 2003; Matsuo and Tanaka, 2004). Figure 4 shows the ratio of covered salt area to total brick surface (Benavente et al., 2004) against to the numbers of the drying/wetting cycles (time).

Experiments performed on mechanism of efflorescence (Benavente et al., 2004; Pel et al., 2003; Hees and Brocken, 2004) reveal that salt profile for the homogenous pore distributed brick can be as Figure 5. This Figure shows that the salt paths growing within this type of bricks are almost randomly flat after the drying/wetting cycles.

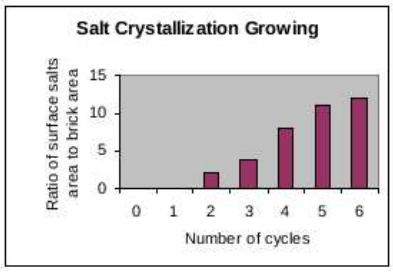


Figure 4: Diagram of salt crystallization growing.

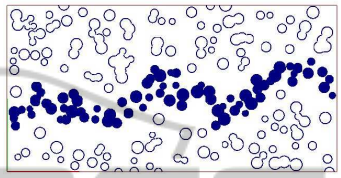

Figure 5: Efflorescence pathway inside the masonry.

Crystallization pressure was first formulated by Correns (Correns, 1949) as follows:

$P = \frac{RT}{V_s} \times \ln \frac{C}{C_s}$

In this equation, $P$ is the pressure exerted by growing crystals in atm, $R$ is the gas constant, $T$ is the temperature in Kelvin, $V_s$ is the molar volume of the solid salt, and $\frac{C}{C_s}$ is the degree of salt super saturation. As our model is limited to physical deteriorations (not chemical), for each point of masonry, we let us propose to calculate the parameter of pressure $P$ according to the density of crystallization around that point (see section 4.3).

## 4 AGING SIMULATION

To obtain an efflorescence pattern, first we adopt a solid texturing method to synthesize a clean masonry. We make a discrete $3D$ block $B$ of colors of size $N^3$ voxels ($N$ is the input texture size). The block $B$ is produced by extruding and perturbing an input $2D$ image patch that represents a view of the desired $3D$ texture. To synthesize masonry, we apply the block of colors $B$ to a masonry silhouette. To add efflorescence we use a potential number $N_p$ and active number $N_d$ of crystal departure points. $N_p$ and $N_d$ physically depend on the porosity $p$ of the material. Table 2 shows

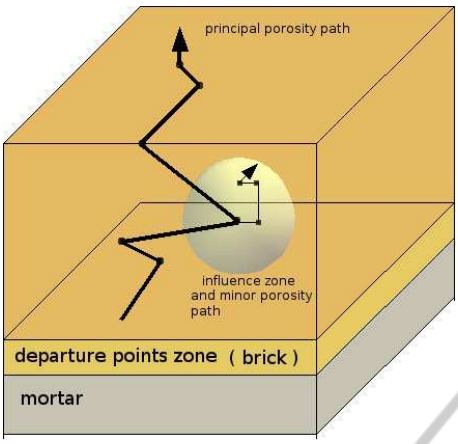


Figure 6: Efflorescence simulation. Starting points that traverse principal porosity path are selected in the preferential zone. Influence zone is used to pore interconnecting.

the density and porosity of the representative type of materials. Generally, porosity of pointing mortar is greater than clay brick porosity.

Table 2: Some characteristics of the masonries. Courtesy from Hees and Brocken (Hees and Brocken, 2004).

| | Density($kg/m^3$) | Porosity(v%) |
|---|---|---|
| Clay brick | 1830 | 32 |
| Pointing mortar | 1670 | 37 |
| Bedding mortar | 2000 | 24 |

We assume homogenous porosity 35 percent for the bricks and mortars (by information given for example in (Pel et al., 1995; Hees and Brocken, 2004)), however user can set it if needed. User can define the starting points zone thickness for the brick; however, this thickness $L_d$ is controlled by system to avoid the problematic errors of limitations and to have the amount of porosity path linked to the brick surface (known as *open porosity*). Starting points can be:

- Selected by user in preferential zones to generate different textures, permitting to provide control of the final results.
- Automatically chosen in the neighborhood of the mortar because mortar acts as the source of salt, penetrating in the brick (Hees and Brocken, 2004; Matsuo and Tanaka, 2004). The starting points for the mortar are distributed all over the mortar volume, because of the homogenous distribution of the salt in the mortar (Figure 6 ). The user can select the type of material and texture (brick or mortar) using the system interface.

Starting points depend on other environmental parameters such as salts present in outside of brick surface and it is difficult to take into account all the parameters. We propose to choose the number of starting points $N_p$ (or $N_d$) as a function of the amount of porosity inside the masonry and the position of each starting point is selected randomly, in the preferential zones. Thus, $N_p$ can be calculated by following equation:

$$N_p = N \times N \times L_d \times p, \qquad 0 \leq L_d \leq N$$

By default, $L_d$ is 5 percent of the brick and whole of the mortar volume size. The active starting points to synthesis a block of color $B$ is:

$$N_d = N_p \times k, \qquad 0.0 \leq k \leq 1.0$$

Where $k$ is a *scale factor* that can also represent the concentration of ions (salt solution viscosity). User sets this parameter empirically (valid between 0.0 and 1.0) in order to obtain the desired results.

## 4.1 Salts Propagation

Efflorescence pathway is random inside the masonry porous structure composed by $T_p$ steps (see section 3). A simple porous structure may be described as the holes connected by the paths (Benavente et al., 2004). These holes and paths are dilated or expanded by the deposited salts. Physically $T_p$ represents efflorescence time quantification in one wetting/drying period. Time quantifying is very difficult as efflorescence has very different diffusion time for each masonry type and for each environment (Ahl, 2003). In addition, many other parameters play a role in salt crystallization on the materials like as thermal conditions. Therefore, in order to handle the time quantification we try just to get the plausible graphical results. At each step of $T_p$, coloring a voxel as crystal element can grow crystallization to the masonry (mortar/brick). To have the continuity of crystallization effect as it is in masonry porous structure, we select some spherical influence zones (randomly selected) for each principal pathway (Figure 6 ). On each influence zone, we have the number $N_s$ of random propagation directions in $P_s$ steps. $N_s$ value as well as $N_p$ (or $N_d$) is related to porosity of masonry. In addition, we consider another parameter $N_c$, to handle repeated wetting and drying cycles of the masonry. One can control the quantity of salt inside the masonry by repeating $T_p$ in $N_c$ cycles.

As we have 26 neighbors for each propagation step voxel, we can choose 10 new sub-propagation directions in influence zone for the fired-clay brick against to its porosity about of 35% ( $26 \times 0.35 \approx 10$).

Influence zone diameter $P_s$ can be limited by occlusion of air in dead-end pores. Having usual porosity distribution between 0.1 and 10 microns (Dorsey

et al., 1999) that is varied with a factor of 100, we consider $P_s = \frac{T_p}{100}$ to keep our model phenomenological. Many porosity path and sub-propagation directions for each step can result in considerable crossing between colored neighborhood points inside the masonry. Table 3 summarize all of these parameters.

## 4.2 Altering Surface Masonry by Efflorescence

To attain a high quality surface alteration we use an adaptive tessellation method of displacement map (Doggett and Hirche, 2000). In this method, displacement features are corresponded to the texture used as the displacement map. These displacement features are used to tessellate the base surface. The adaptive tessellation produces fewer triangles than the methods use uniform subdivision of the base surface. We define a *positive displacement* as the elevation and *negative displacement* as depression. Displacement offset correspond to the grey level colors from black to white (neutral grey means no displacement).

To have an elevated surface attacked by salt crystals we adopt the grey level image of each masonry view as a *positive displacement map*. In addition, to control the height of the displacement we define a scale factor $H_d$ valid in the range [0, 1]. Figure 7 compares a real and two synthesized aged bricks using usual bump and displacement map methods.

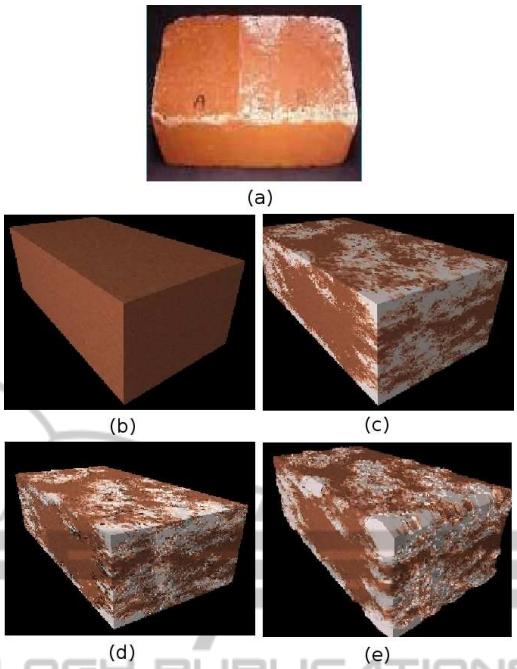


Figure 7: (a) A real brick efflorescence. (b) A synthesized clean brick, (c) The brick affected by efflorescence without change of geometry. (d) Bump mapping method to alter the surface. (e) Displacement map method to alter the surface. Here: N = 128, p = 0.3, $N_s = 8(26 \times p)$, $N_c = 10$, $L_d = 2$, $N_p = (N \times N) \times p \times L_d = 9830$, k = 0.03, $N_d = 294$, $T_p = 300$, $P_s = 3(T_p/100)$, $H_d = 0.2$. Note that brick in image (d) has artifacts in its border.

## 4.3 Masonry Surface Erosion (Spalling)

The depth of damage generally depends on the brick quality, crystallization, drying/wetting cycles, quantity of masonry porosity and water suction. Because of the model limitations that is not completely volumetric i.e., our model is based on mesh grid of the object, we do not have all the information of the zone underneath affected by sub-florescence. Then, we cannot have a complete quantification of damage. However, we know that efflorescence can be an advanced sub-florescence moved toward the surface by open porosity. Therefore, we can define a function $f$ to compute the quantity (depth) of damage over the parts of masonry that have been attacked by efflorescence:

$D = f(P,H)$

Here $P$ is the pressure exerted by growing crystals; $H$ is the distance of underneath point from the exterior surface. We assume that enough high crystal density can produce pressure enough to alter the image of point along the normal vector to the surface. This assumption is valid for the aged masonry (Bucea et al., 2005; Nehdi and Hayek, 2005). So at each point of masonry the density of salt crystallization can present its exerted pressure. Then, to calculate the parameter $P$ at each point, we can calculate the density of crystallization around this point. The depth of damage is depending on the $H$, i.e., higher value of $H(H \approx 1.0)$ can damage the surface deeply over time. Note that we consider all the crystallization grain, underneath near enough the exterior face to have a regular alteration. Function $f$ has a direct relation with $P$ and $H : P \times H$ or $(P \times H)/c$ for example, where $c$ is a scale factor.

To synthesize a crumbled surface, we apply the method presented in section 4.2 but with some differences. Here, we use a *Negative displacement map* to alter the surface masonry. In addition, efflorescence texture assignment can be chosen by user tact. This is because on a masonry surface the efflorescence can be absent or different from those on eroded areas.

Figure 8(b) represents a synthesized eroded brick.

## 4.4 Problem of Very Hard Alteration

To handle the very hard alteration of masonry facade (Figure 9) we propose to alter the masonry mesh before its rendering.

Table 3: Summary of efflorescence simulation parameters.

| Parameter | Description | Range Value | Phenomenological Meaning |
|---|---|---|---|
| $N$ | solid texture size | masonry image size (pixel) | - |
| $p$ | porosity of the masonry | typically between 0.24 and 0.40 | porosity |
| $k$ | scale factor of departure points | between 0.0 et 1.0 | viscosity scaling |
| $N_p$ | potential departure points | between 0 and $N^3 \times p$ | water soluble penetrating |
| $N_d$ | active number of departure points | between 0 et $N^3 \times p \times k$ | solution viscosity |
| $T_p$ | principle propagation walks | graphical result (between 0 and $N^3$) | drying/wetting cycles |
| $N_s$ | number of random directions | $26 \times p$ ( by default 10) | influence zone driven |
| $P_s$ | sub-propagation walks | $T_p/100$ | pore interconnection |
| $H_d$ | efflorescence depth | between 0.0 and 1.0 | damage scaling |
| $N_c$ | number of cycles | $N_c \geq 1$ | repeating $T_p$ |
| $L_d$ | departure points zone | $0 \leq L_d \leq N$ for brick, $L_d = N$ for mortar | mortar humidity thickness |



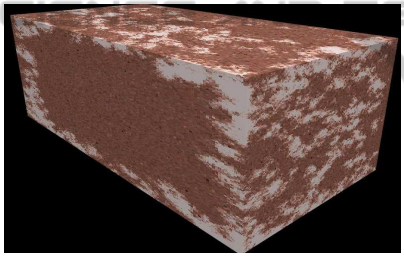

(a)

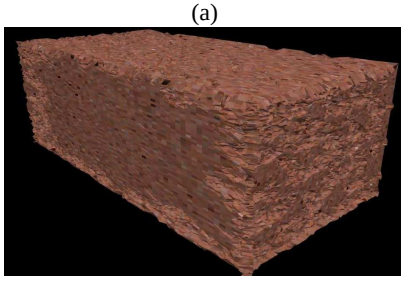

(b)

Figure 8: (a) A synthesized efflorescence brick without alteration (b) An eroded synthesized brick ; to obtain this eroded clay brick we use a negative displacement map with eliminating the efflorescence color. The weathering parameters are as well as Figure 7. Damage depth $D = f(P,H) = P \times H$.

Figure 9: An example of very strong surface alteration.

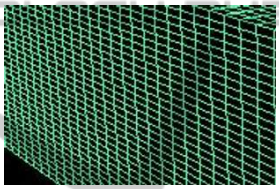

(a) A brick mesh subdivision.

(b) A texture model.

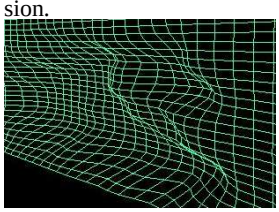

(c) Deforming the mesh.

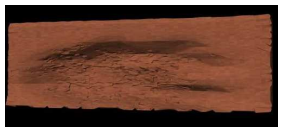

(d) Rendering result.

Figure 10: Mesh alteration processes. Here to further visibility the brick mesh is too subdivided, in practice $15 \times 15 \times 15$ subdivision is sufficient.

First task is to subdivide base mesh model just enough high to the some cubical parts (for example $15 \times 15 \times 15$ cubes for each brick). Then to have a deformation effect, we simply use an efflorescence texture corresponding to the displacement offset desired (Figure 10). After these processes we have the deformed masonry to which one can apply the method presented in the preceding section ( 4.3) to carry out very strong crumbling. Here, texture used for geometry deformation is the same one as the texture used for displacement map.

(a) (b)

Figure 11: (a) A real stone-pavement image. (b) Synthesized image.

## 5 RESULTS

We were interested to generate wide variety of salts decay aging of bricks. Aliasing artifacts are the common problem of textures that are present unfortunately also for solid textures. In order to improve image quality we integrate an antialiasing filtering process in the system. There are generally two methods of doing antialiasing, super-sampling, and edge antialiasing. Super-sampling antialiasing method renders the scene in a much high resolution and then scale down to the original size. This way, the scene will be approximated and the staircase edges will disappear. This method is simple but requires an accelerator of very high fill-rate. Edge antialiasing calculates all edges and their surrounding polygons to find out the best color for the edge pixels. This calculation is highly CPU-intensive and is rarely done in consumer-level 3D accelerators. As the system presented in this paper is not restricted to real-time rendering, i.e., texture synthesis computation time is less than one second and synthesis time for a construction with 1000 bricks using an Intel DUO 3.0 GHZ is about 15 minutes (with $N = 64$), this gives us the freedom to use edge antialiasing method.

Figure 11 illustrates a comparison of a real stone-pavement image and synthesized one. Each brick behaves independently, depending on numerous parameters. Figure 12 illustrates a synthesized landscape by different degree of efflorescence and erosion. To generate such virtual construction, user can instantiate each brick and define its position, then he can texture it by a great variety of solid texture. Two examples of very hard erosion on brick walls are shown in Figure 13.

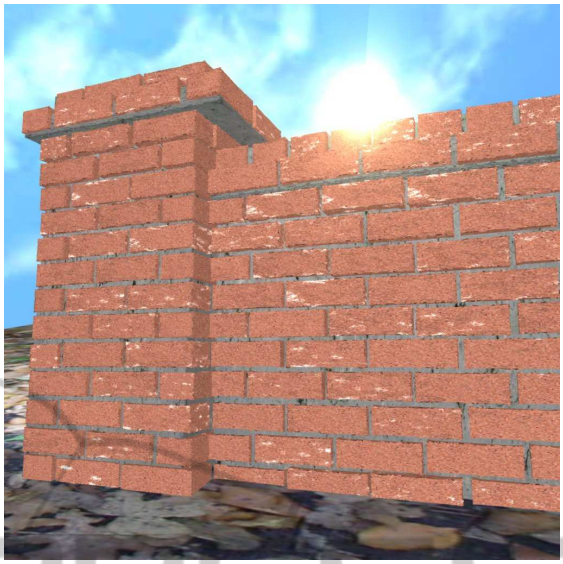

Figure 12: Synthesized landscape.

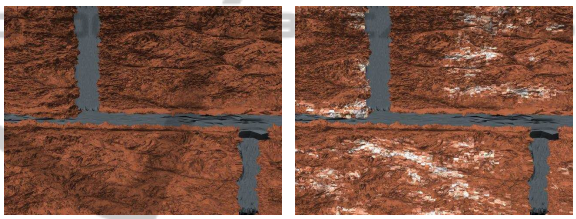

Figure 13: Very hard brick surface erosion.

## 6 CONCLUSIONS AND FUTURE WORK

This paper presents improvements and solutions to the issues unsolved in former work (Shahidi et al., 2005). We have used the same 3D texture model to synthesize efflorescence color on masonry, by adding other different visual aspects as geometry modification and mechanical damage. The method is physically inspired and is simple to implement as it is based on well-known solid texture and displacement map. Furthermore, the system provides a good computation time (Table 4). While the results are plausible and can cover common weathering phenomena, we feel there are several possibilities for future work. An important future work is to generate the 3D texture in a narrow region around the boundary of the solid texture. This improvement not only can speed up the calculation process of texture synthesis, but also can decrease the memory requirements.

Another possible improvement is to sculpt the facade of construction. We handled it by a geometri-

Table 4: A representative table of times (in minute) for rendering some results. Note that for all particles (brick/mortar) in these figures we have the unique initial subdivision mesh (equal triangle number).

| - | $N^3$ | Particle number | Time |
|---|---|---|---|
| Figure 11 | $128^3$ | 237 | 31 |
| Figure 12 | $128^3$ | 226 | 30 |

cal model before rendering the object. However, we believe using a volumetric model is preferred, as it can directly perturb the surface without need to further texturing process. In addition, by the volumetric modeling other weathering phenomena as the salts present very dens on the surface, crack, etc. will be easier to handle; hence, in future we envisage working on it.

Our current implementation allows the user manually position and texture each brick separately, we can improve this system to automatic positioning and add the weathering aspect according to wall location. For this, one can use the environment parameters as humidity, salt degree, porosity, etc.

We have assumed that the masonry has a homogeneous structure, however it is not common and there are inhomogeneous aspects inside the masonry that can change weathering effects. This problem should be considered.

## REFERENCES


Ahl, J. (2003). Salt diffusion in brick structures. In *Journal of Materials Science*, volume 38, pages 2055–2061.

Becket, W. and Badler, N. (1990). Imperfection for realistic image synthesis. In *Journal of Visualization and Computer Animation*, volume 1, pages 26–32.

Benavente, D., Garcia, M., Garcia-Guinea, J., Sanchez-Moral, S., and Ordonez, S. (2004). Role of pore structure in salt crystallisation in unsaturated porous stone. In *Journal of Crystal Growth*, volume 260, pages 532–544.

Blinn, J. F. (1982). Light reflection functions for simulation of clouds and dusty surfaces. In *Computer Graphics*, volume 3, pages 21–29.

Bosch, C., Merillou, S., Pueyo, X., and Ghazanfarpour, D. (2004). A physically-based model for rendering realistic scratches. In *Computer Graphics Forum*, volume 23, pages 361–370.

Bucea, L., Khatri, R., and Sirivivatnanon, V. (2005). Chemical and physical attack of salts on concrete. In *Proceedings Urban Salt 2005 Conference*.

Correns, C. (1949). Growth and dissolution of crystals under linear pressure. In *Discussions of the Faraday Society*, volume 5, pages 267–71.

Cutler, B., Dorsey, J., McMillan, L., Muller, M., and Jagnow, R. (2002). A procedural approach to authoring solid models. In *ACM Transaction on Graphics (TOG)*, volume 21, pages 302–311.

Desbenoit, B., Galin, E., and Akkouche, S. (2004). Simulating and modeling lichen growth. In *Computer Graphics Forum*, volume 23, pages 361–370.

Doggett, M. and Hirche, J. (2000). Adaptive view dependent tessellation of displacement maps. In *SIGGRAPH/Eurographics Workshop on Graphics Hardware*, pages 59–66.

Dorsey, J., Edelman, A., Jensen, H., Legakis, J., and Pedersen, H. (1999). Modeling and rendering of weathered stone. In *ACM SIGGRAPH*, pages 225–234.

Dorsey, J. and Hanrahan, P. (1996). Flow and changes in appearance. In *ACM SIGGRAPH*, pages 411–420.

Hees, R. and Brocken, H. (2004). Damage development to treated brick masonry in a long-term salt crystallisation test. In *Construction and Building Materials*, volume 18, pages 331–338.

Hsu, S. and Wong, T. (1995). Simulating dust accumulation. In *IEEE Computer Graphics and Applications*, volume 15, pages 18–22.

Huinink, H., Pel, L., and Michels, M. (2002). How ions distribute in a drying porous medium-a simple model. In *Phys Fluids*, volume 14, pages 1389 –1395.

Lu, J., Georghiades, A., Glaser, A., Wu, H., Wei, L.-Y., Guo, B., Dorsey, J., and Rushmeier, H. (2007). Context-aware textures. In *ACM Trans. Graph.*, volume 26, pages 167–174.

Matsuo, T. and Tanaka, K. (2004). Mechanism of efflorescence on historical brick masonry buildings reinforced with concrete. In *Proceedings of 10th International Conference on Durability of Building Materials and Components*, pages 1–8.

Merillou, N., Merillou, S., Ghazanfarpour, D., Dischler, J., and Galin, E. (2010). Simulating atmospheric pollution weathering on buildings. In *WSCG*, pages 65–72.

Merillou, S., Dischler, J.-M., and Ghazanfarpour, D. (2001). Corrosion: Simulating and rendering. In *Graphics Interface*, pages 167–174.

Merillou, S. and Ghazanfarpour, D. (2008). A survey of aging and weathering phenomena in computer graphics. In *Computer Graphics*, volume 32, pages 159–174.

Miller, G. (1994). Efficient algorithms for local and global accessibility shading. In *ACM SIGGRAPH*, volume 21, pages 319–326.

Nehdi, M. and Hayek, M. (2005). Behavior of blended cement mortars exposed to sulfate solutions cycling in relative humidity. In *Cement and Concrete Research*, volume 35, pages 731–742.

Paquette, E., Poulin, P., and Drettakis, G. (2001). Surface aging by impacts. In *Graphics Interface*, pages 175–182.

Paquette, E., Poulin, P., and Drettakis, G. (2002). The simulation of paint cracking and peeling. In *Graphics Interface*, pages 59–68.

Peachey, D. R. (1985). Solid texturing of complex surface. In *Computer Graphics*, pages 279–286.

Pel, L., Huinink, H., and K.Kopinga (2003). Salt transport and crystallization in porous building materials. In *Magnetic Resonance Imaging*, volume 21, pages 317–320.

Pel, L., Huinink, H., Kopinga, K., van Hees, R., and Adan, O. (2004). Efflorescence pathway diagram: understanding salt weathering. In *Construction and Building Materials*, volume 18, pages 309–313.

Pel, L., Kopinga, K., Bertram, G., and Lang, G. (1995). Water absorption in fired-clay brick observed by nmr scanning. In *J. Phys. D: Appl. Phys.*, volume 28, pages 675–680.

Perlin, K. (1984). A unified texture/reflectance model. In *SIGGRAPH 84 Advanced Image Synthesis course notes*.

Perlin, K. (1985). An image synthesizer. In *Computer Graphics*, volume 19, pages 287–296.

Shahidi, S., Merillou, S., and Ghaznanfarpour, D. (2005). Phenomenological simulation of efflorescence in brick constructions. In *Proceedings of Eurographics on Natural Phenomena*, volume aug, pages 17–23.

Wong, T., Ng, W. Y., and Heng, P. A. (1997). A geometry dependent texture generation framework for simulating surface imperfections. In *Proceedings of Eurographics Workshop on Rendering*, pages 139–150.